

## Ferromagnetic resonance spectroscopy of parametric magnons excited by a four-wave process

V. V. Naletov,<sup>1,2</sup> G. de Loubens,<sup>1</sup> V. Charbois,<sup>1</sup> O. Klein,<sup>1</sup> V. S. Tiberkevich,<sup>3</sup> and A. N. Slavin<sup>3</sup>

<sup>1</sup>*Service de Physique de l'État Condensé (CNRS URA 2464), CEA Saclay, 91191 Gif-sur-Yvette, France*

<sup>2</sup>*Physics Department, Kazan State University, Kazan 420008, Russia*

<sup>3</sup>*Department of Physics, Oakland University, Michigan 48309, USA*

(Received 12 January 2007; revised manuscript received 16 March 2007; published 24 April 2007; publisher error corrected 25 April 2007)

Using a magnetic resonance force microscope, we have performed ferromagnetic resonance spectroscopy of the parametric magnons created by a four-wave process. This is achieved by measuring the differential response to a small amplitude modulation superimposed to a large constant excitation power that drives the dynamics of the uniform mode in the saturation regime. By sweeping the applied field, we observe an abrupt readjustment of the total number of magnons each time the excitation coincides with a parametric mode. This gives rise to ultranarrow peaks whose linewidth is lower than  $5 \times 10^{-6}$  of the applied field.

DOI: [10.1103/PhysRevB.75.140405](https://doi.org/10.1103/PhysRevB.75.140405)

PACS number(s): 76.50.+g

The detailed understanding of the nonlinear (NL) regime of the magnetization dynamics is important both from a fundamental point of view<sup>1</sup> but also for applications in spintronic devices.<sup>2</sup> Interest resides in the exact nature of the parametric modes that are excited above the supercriticality threshold. Recent experiments performed on a yttrium iron garnet (YIG) film have shown that these parametric magnons can form a Bose-Einstein condensate<sup>3</sup> under high power pumping. It was also demonstrated that the energy decay rate of parametric modes is substantially diminished compared to the long-wavelength modes,<sup>4</sup> which are usually studied by ferromagnetic resonance (FMR). It will be shown that it is possible to measure the spectrum of parametric magnons despite the fact that these high  $k$ -vector spin-waves (SWs) do not couple directly to an homogeneous microwave excitation field  $h$ . This is achieved by saturating the dynamics of the uniform mode through a large constant microwave power and superposing onto it an additional power source. The additional energy injected in the spin system excites indirectly the parametric magnons. Since each parametric mode has a different feedback influence on the saturation mechanism, it is possible, by sweeping an external parameter, to detect the point where the transfer from one parametric mode to another one takes place. Because the induced effects are small, detecting them requires both a sensitive and precise measurement setup.

We use here an original and sensitive detection method to study the spin-wave spectrum: a mechanical-FMR setup working at room temperature.<sup>5,6</sup> Although the detection scheme is inspired by local probe techniques, the excitation scheme still uses a microwave antenna to induce a precession of the spontaneous magnetization  $M_s$  by canting it away from its equilibrium axis by an angle  $\alpha$ . The mechanical instrument measures the longitudinal component of the magnetization,  $M_z = M_s \cos \alpha$ , which is coupled through the dipolar interaction to a magnetic probe attached at the end of a soft cantilever. Exciting the sample at a fixed frequency, spectroscopy is achieved by recording the cantilever motion as a function of the perpendicular dc applied field  $H_{\text{ext}}$  produced by an electromagnet. The variation of the force on the cantilever is proportional to the total number of magnons excited at resonance,  $N_t \equiv (M_s - M_z) / (\gamma \hbar)$ . Further details about the experiment can be found in Ref. 7.

Driving the dynamics of ferromagnets in the NL regime requires us to cant  $M_s$  by an angle  $\alpha$  exceeding a couple of degrees. Only a powerful hyper-frequency (HF) source can produce a large enough excitation amplitude.<sup>8</sup> Improvement of the efficiency can be gained with microstrip cavities, where the HF energy is concentrated in a smaller volume. A schematic of our setup is shown in Fig. 1(a). It comprises a 500- $\mu\text{m}$ -wide Au stripline fabricated by UV lithography and deposited on a 500- $\mu\text{m}$ -thick alumina substrate with a bottom conducting ground plane. An impedance matched cavity (half wavelength) is created by etching a 32- $\mu\text{m}$  gap across the stripe. The HF source is tuned at the cavity frequency ( $\omega_s / 2\pi = 10.47$  GHz) set by the length (5 mm) of the isolated segment. The sample is a  $t = 4.75$ - $\mu\text{m}$ -thick YIG single crystal, ion milled into a disk of diameter  $\phi = 160$   $\mu\text{m}$ . It is placed at the center of the cavity. The homogeneous external static field  $H_{\text{ext}}$ , well above the saturation field, is applied parallel to the disk axis.

This work concentrates on the four-magnon coupling term in the equation of motion of the magnetization. It becomes the dominant term once the premature saturation regime of the microwave susceptibility is achieved.<sup>9</sup> From previous experiments on the same sample,<sup>4</sup> we have established that the saturation threshold occurs at excitation power above  $P_{cr} = -22$  dBm for our setup. Figure 1(b) shows the static deflection of the cantilever as a function of  $H_{\text{ext}}$  when the excitation power is  $-10.8$  dBm. The trace corresponds to the line shape of the uniform mode<sup>10</sup> in the foldover regime. Hysteretic behaviors are a standard signature of NL effects, where the eigenfrequency of the resonance depends on the amplitude of the excitation.<sup>11</sup> Foldover effects in magnetic materials have been explained by Anderson and Suhl in 1955.<sup>12</sup> The features of interest are the tiny steps observed in the wings of the resonance [cf. inset of Fig. 1(b)]. These jumps are not random. They are reproducible and occur regularly in field.

A more detailed picture can be obtained by measuring the differential response. We detect here the response to an amplitude modulated excitation around the saturation regime. The power level writes  $P(t) = P_{\text{max}} \{1 + \frac{\epsilon}{2} [\sin(\omega_c t) - 1]\}$ , where the modulation frequency is set at the resonance frequency of the cantilever. This frequency is much lower than all the

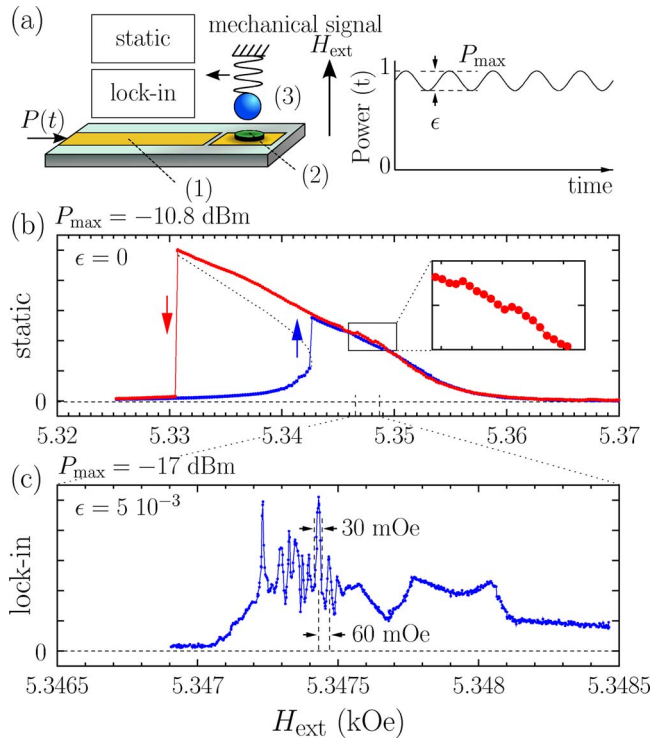


FIG. 1. (Color online) (a) Schematic of the microstrip cavity (1). The FMR spectrum of a micron-size YIG disk (2) is detected mechanically by magnetic resonance force microscopy (3). On the right is shown  $P(t)$ , the waveform of the power injected in the microwave circuit (1). (b) Static deflection of the cantilever as a function of  $H_{\text{ext}}$ . The trace is the line shape of the uniform mode in the foldover regime. (c) Vibration amplitude of the cantilever measured by a lock-in synchronous with the amplitude modulation. This differential characteristic reveals the parametric excitation spectrum.

damping rates of the spin system. Thus the differential part of the mechanical signal is amplified by  $Q=4500$ , the quality factor of the mechanical resonator. Figure 1(c) is the pattern recorded by a lock-in when the modulation amplitude is 0.5% ( $\epsilon=5 \times 10^{-3}$ ) of the maximum power,  $P_{\text{max}}=-17$  dBm. It corresponds to a modulation of less than 50 nW in amplitude. The spectrum shown here is a zoom on a 2-Oe window of  $H_{\text{ext}}$  in the reversible region of the static signal. We observe about ten ultranarrow lines (width 30 mOe) regularly spaced every 60 mOe. Such sharp peaks resemble the parametric excitations observed by Jantz and Schneider in 1975 in the subsidiary absorption of YIG films<sup>13</sup> (three-wave process). To the best of our knowledge, this is, however, the first time that they are observed at resonance.

The striking characteristic of these peaks is their narrowness. The 30-mOe broadening is much smaller than the FMR linewidth  $\Delta H=1.2$  Oe measured in the linear regime on the same sample.<sup>14</sup> Further insight can be obtained by looking at the shape of the signal [cf. Fig. 2(a) for different modulation depth  $\epsilon$  at constant maximum power  $P_{\text{max}}$ ]. Figure 2(b) shows the broadening  $B$  (width at half maximum) of the isolated parametric mode indicated by the triangle. We find that  $B$  is clearly proportional to  $\epsilon$ . Foldover effects establish a coupling between the HF power and the resonance fre-

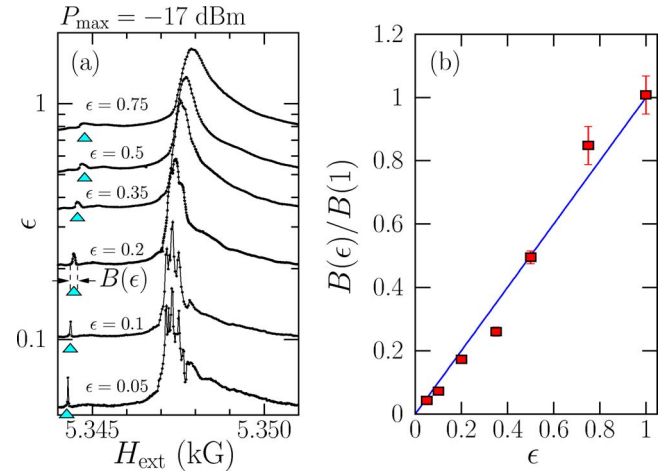


FIG. 2. (Color online) (a) Differential spectrum as a function of the modulation depth  $\epsilon$ , when  $P_{\text{max}}=-17$  dBm is kept constant.  $B$  is the broadening of the isolated parametric peak indicated by the triangle. (b)  $B$  as a function of  $\epsilon$ .

quency. Thus amplitude modulation in the NL regime also produces a modulation of the resonance frequency. In the perpendicular geometry, there is no difference between a frequency modulation and a modulation of the applied field, since both are coupled by the gyromagnetic ratio. Figure 1(c) can thus be seen as the differential characteristics of Fig. 1(b), where the depth of modulation is proportional to  $\epsilon$ . At very low  $\epsilon$  the intrinsic broadening should eventually be observed. Although a NMR electromagnet with a  $10^{-6}$  precision in  $H_{\text{ext}}$  has been used, the fact that  $B$  linearly extrapolates down to the smallest value of  $\epsilon$  reached by our setup suggests that the intrinsic part of the broadening has not been measured. We recall here that SW modes are collective motion and that there is no link between the observed broadening and the homogeneity of the effective field, in contrast to paramagnets. Fundamental mechanisms responsible for the intrinsic broadening will be discussed below.

For completeness, Fig. 3 shows how the instability region evolves when the dc bias  $P_{\text{max}}$  is increased at constant  $\epsilon$ . We observe a spreading of the window of the applied field where the parametric peaks occur. It monotonically follows the magnitude of the power, i.e., how far we depart from the supercriticality threshold.

In the following, we propose an analytical framework to account for the main features observed experimentally. Saturation phenomena can be caused by a multitude of NL processes: NL dissipation, NL phase mechanism, NL energy feedback effect.<sup>11</sup> In many cases several of these mechanisms, as well as NL frequency shift, need to be simultaneously accounted for the correct description of the phenomenon. The most probable limiting mechanism in the case of perpendicular pumping is the NL energy feedback. It coherently couples degenerate SWs of equal and opposite wave vectors  $(+k, -k)$ .<sup>9</sup> Two quanta of the uniform precession break down in a parametric magnon pair propagating along the magnetization direction. The instability corresponds to a

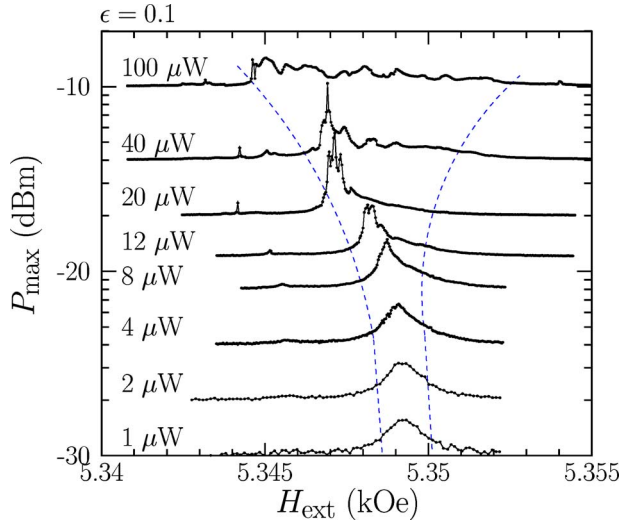


FIG. 3. (Color online) Differential spectrum as a function of  $P_{\max}$ . In this set of measurement,  $\epsilon$  is kept constant at  $\epsilon=0.1$ .

spatial distortion of the instantaneous axis of precession which diminishes the transverse demagnetizing energy. This mechanism is described by a four-magnon term ( $\xi_k b_0^2 b_k^* b_{-k} + \text{c.c.}$ ) in the Hamiltonian of the system. It represents the second-order parametric excitation of the pair of plane SW ( $b_k, b_{-k}$ ) by the uniform precession ( $b_0$ ). Suhl showed in 1957 that the equations of motion for the amplitudes  $b_k$  have the form

$$\dot{b}_k = -i\omega_k b_k - i\xi_k b_0^2 b_{-k}^* - \eta_k b_k, \quad (1)$$

where  $\eta_k$  is their energy decay to the lattice (the index must allow for  $k$ -dependent relaxation rates<sup>4,15</sup>). The equation for the amplitude  $b_0$  of the uniform precession is given by

$$\dot{b}_0 = -i\omega_0 b_0 - i \sum_k \xi_k b_k b_{-k}^* - \eta_0 b_0 + \gamma h e^{-i\omega_s t}, \quad (2)$$

where the last term is the excitation field rotating at  $\omega_s$ . The term  $\sum_k \dots$  describes the NL feedback effect of all the parametric SWs on the uniform precession. In the following, we will be looking at harmonic solutions where all the SWs precess synchronously:  $\dot{b}_k = -i\omega_s b_k$ .

As one can see from Eq. (1), an instability (exponential growth of the population) occurs if the effective damping of at least one parametric mode becomes negative:

$$|b_0|^4 > \frac{(\omega_k - \omega_s)^2 + \eta_k^2}{\xi_k^2}. \quad (3)$$

The growth of  $b_k$  creates an effective damping for the uniform mode [through the  $\sum_k \dots$  term in Eq. (2)], which reduces  $b_0$  to its threshold value:

$$|b_0|^2 = N_0 \equiv \min_k \frac{\sqrt{(\omega_k - \omega_s)^2 + \eta_k^2}}{\xi_k}, \quad (4)$$

where  $N_0$  is the number of uniform magnons above the supercriticality threshold. The determination of the mode that will grow unstable depends on the coupling  $\xi_k$ , which is

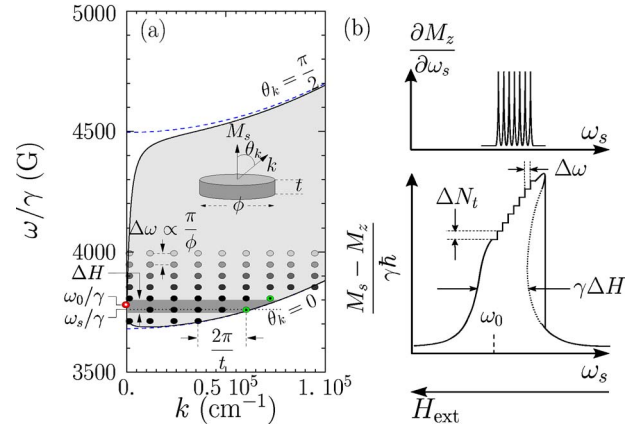


FIG. 4. (Color online) (a) Magnon manifold for our perpendicularly magnetized YIG disk. The shaded area represents the trade-off between exchange energy, increasing with  $k$ , and demagnetizing energy, decreasing with the angle  $\theta_k$  between  $\mathbf{k}$  and  $\mathbf{M}_s$  ( $0 \leq \theta_k \leq \pi/2$ ). The confinement by the finite size of the sample introduces a discretization of the normal modes (dots). The four-wave process couples the uniform mode (red dot with white center) to the parametric modes at  $\theta_k \approx 0$  (green dots with black centers) (b) Schematic of the distortion of the line shape induced by the four-wave process: the staircase behavior of  $(M_s - M_z)/(\gamma\hbar) = \sum_k N_k$  reveals the parametric spectrum in the differential characteristics  $\partial M_z / \partial \omega_s$ .

maximum ( $\xi_k / \gamma = 2\pi M_s \approx 900$  G) for the propagation wave vector parallel to  $\mathbf{M}_s$ .<sup>9</sup> As shown on the magnon manifold drawn in Fig. 4(a), these longitudinal SWs have a wave vector  $k_{\max} = \sqrt{N_{\perp} 4\pi M_s^2 / (2A)} \approx 6.3 \times 10^4 \text{ cm}^{-1}$ , where  $A$  is the exchange constant and  $N_{\perp}$  is the transverse depolarization factor. For our disk, it corresponds to a standing SW confined across the thickness with about five nodes along it. In this model, the threshold power is given by the analytical formula  $h_{cr}^2 = \eta_k \Delta H^2 / \xi_k$ , where the onset of saturation  $h_{cr} = 5$  mOe has been established experimentally.<sup>4</sup>

Sweeping the bias magnetic field  $H_{\text{ext}}$  (or  $\omega_s$ ) changes the nature of the parametric mode that grows unstable, as the minimum in Eq. (4) occurs for different values of  $k$ . Finite-size effects introduce a discretization in  $k$  space of all the SWs. The frequency separation  $\Delta\omega$  between two nearby normal modes is about  $\Delta\omega = 4\gamma A k \Delta k / M_s$ , where  $\Delta k = \pi / \phi$  corresponds to the quantification of the  $k$  vector along the largest sample dimension. The parametric modes have thus a principal wave vector  $\mathbf{k}_{\max} \parallel \mathbf{M}$ , with a small additional component  $\Delta\mathbf{k}$  in the disk plane. We find numerically  $\Delta\omega / \gamma = 0.12$  Oe, a predicted separation twice as large as what is observed experimentally in Fig. 1(c). However, the value of  $k_{\max}$  strongly depends on the angle of propagation of the degenerate magnons. A deviation of about  $7^\circ$  of their propagation direction compared to the normal of the disk would be enough to explain the discrepancy.

The amplitude of the steps can also be estimated analytically with an approximated model. Assuming that only one pair of parametrically coupled SWs dominates all the others, then its amplitude can be inferred from Eq. (2). If the mode  $b_k$  is dominant, its amplitude will grow to the level

$$|b_k|^2 = |b_{-k}|^2 = N_k \equiv \frac{\sqrt{(\gamma h)^2 \xi_k^2 N_0 - \{(\omega_k - \omega_s) \eta_0 + (\omega_0 - \omega_s) \eta_k\}^2 + (\omega_0 - \omega_s)(\omega_k - \omega_s) - \eta_0 \eta_k}}{N_0 \xi_k^2}, \quad (5)$$

that provides the effective damping to fix  $N_0$  at the level given by Eq. (4). The number of magnons in the majority mode  $N_k$  abruptly changes with the change of the excited mode due to the sweep of the magnetic field. In the differential graphs this will lead to a singularity at the points where the transfer from one excited mode to another one takes place. In reality, due to the presence of thermal noise and of other NL processes (that are ignored here) one will observe a sharp (intrinsically broaden) peak.

To see this more clearly, let us assume that the coupling coefficients of all the modes are the same,  $\xi_k = \xi$ . We assume here that one sweeps the frequency ( $M_z$  vs  $\omega_s$ ). The line-shape distortion directly maps onto a mechanical-FMR spectrum ( $M_z$  vs  $H_{\text{ext}}$ ) through the effective gyromagnetic ratio [see Fig. 4(b)]. The changes of the parametrically excited modes (say, modes 1 and 2) will be at such a magnetic field that  $(\omega_1 - \omega_s) = -(\omega_2 - \omega_s) = \Delta\omega/2$  [cf. Eq. (4)]. Assuming that  $|\omega_0 - \omega_s| \ll \eta_k$  and  $\Delta\omega \ll \eta_k$  we can write  $N_0 \approx \eta_k / \xi$  and, approximately,

$$N_{1,2} \approx (\zeta - 1) \frac{\eta_0}{\xi} \pm \frac{(\zeta - 1)}{\zeta} \frac{(\omega_0 - \omega_s) \Delta\omega}{2\xi\eta_k}, \quad (6)$$

where  $\zeta \equiv h/h_{\text{cr}}$  is the supercriticality parameter of the microwave magnetic field. Thus the total number of SW modes differs by

$$\Delta N_t \equiv N_1 - N_2 = \frac{(\zeta - 1)}{\zeta} \frac{(\omega_0 - \omega_s) \Delta\omega}{\xi\eta_k}. \quad (7)$$

As shown in Fig. 4(b) this creates small “steps” (of the order of 1% of  $N_t$ ) in the line shape at different “integral” characteristics and ultranarrow peaks at “differential” characteristics of  $M_z$  vs  $H_{\text{ext}}$ . These analytical findings are in good agreement with the experimental ones observed in Fig. 1.

In summary, we have performed FMR spectroscopy of parametric magnons. Future research direction would be the measurement of the intrinsic linewidth of these parametric resonances, but it would require an extremely sensitive spectrometer. The extreme narrowness of the peaks observed, already opens up the possibility of making ultrastable YIG tuned oscillators or ultrasensitive magnetic-field sensors capable to compete with NMR probes.

<sup>1</sup>A. N. Slavin and V. S. Tiberkevich, Phys. Rev. B **74**, 104401 (2006).

<sup>2</sup>G. A. Prinz, J. Magn. Magn. Mater. **200**, 57 (1999).

<sup>3</sup>S. O. Demokritov, V. E. Demidov, O. Dzyapko, G. A. Melkov, A. A. Serga, B. Hillebrands, and A. N. Slavin, Nature (London) **443**, 430 (2006).

<sup>4</sup>G. de Loubens, V. V. Naletov, and O. Klein, Phys. Rev. B **71**, 180411(R) (2005).

<sup>5</sup>Z. Zhang, P. C. Hammel, and P. E. Wigen, Appl. Phys. Lett. **68**, 2005 (1996).

<sup>6</sup>V. Charbois, V. V. Naletov, J. Ben Youssef, and O. Klein, Appl. Phys. Lett. **80**, 4795 (2002).

<sup>7</sup>V. V. Naletov, V. Charbois, O. Klein, and C. Fermon, Appl. Phys.

Lett. **83**, 3132 (2003).

<sup>8</sup>S. Y. An, P. Krivosik, M. A. Kraemer, H. M. Olson, A. V. Nazarov, and C. E. Patton, J. Appl. Phys. **96**, 1572 (2004).

<sup>9</sup>H. Suhl, J. Phys. Chem. Solids **1**, 209 (1957).

<sup>10</sup>V. Charbois, V. V. Naletov, J. Ben Youssef, and O. Klein, J. Appl. Phys. **91**, 7337 (2002).

<sup>11</sup>V. S. L'vov, *Wave Turbulence Under Parametric Excitation* (Springer, Berlin, 1994).

<sup>12</sup>P. W. Anderson and H. Suhl, Phys. Rev. **100**, 1788 (1955).

<sup>13</sup>W. Jantz and J. Schneider, Phys. Status Solidi A **31**, 595 (1975).

<sup>14</sup>O. Klein, V. Charbois, V. V. Naletov, and C. Fermon, Phys. Rev. B **67**, 220407(R) (2003).

<sup>15</sup>U. Hoeppe and H. Benner, Phys. Rev. B **71**, 144403 (2005).